

# Hydrothermal Synthesis of Cobalt Disulfide Nanostructures and Adsorption Kinetics, Isotherms, and Thermodynamics of Tetracycline

Mohammad Javad Aghagoli and Farzaneh Shemirani\*

Department of Analytical Chemistry, College of Science, University of Tehran, Tehran, Iran.

(\*) Corresponding author: shemiran@khayam.ut.ac.ir  
(Received: 21 August 2017 and Accepted: 25 August 2019)

## Abstract

Surfaces of synthesis cobalt disulfide has high electron density that could interact with polycyclic aromatic compounds by  $\pi$ - $\pi$  stacking. Cobalt disulfide was synthesized with the hydrothermal method and characterized by field emission scanning electron microscopy, X-ray diffraction and energy-dispersive X-ray. Using tetracycline as a model analyte, the batch adsorption experiments were carried out in order to investigate the adsorption capacity of the adsorbent. It was revealed that pseudo-second-order kinetic model can better describe the adsorption kinetic. Furthermore, the equilibrium adsorption data were congruous with the model Langmuir with maximum adsorption capacity of  $163.93 \text{ mg g}^{-1}$ .

**Keywords:** TC determination, Agricultural water, Spectrophotometry.

## 1. INTRODUCTION

Pharmaceutical products have become the center of much current environmental researches. Groundwater pollution by pharmaceutical ingredients is an environmental problem of widespread concern. Pharmaceutical ingredients are actually found as residues in water and have recognized as a part of the hazardous chemical substances able to alter the natural equilibrium system of the surrounding environment [1, 2]. Antibiotics are widely used as infectious disease medicines, which have become a serious problems as they have variety of potential adverse effects, including impact on photosynthetic organisms, acute toxicity, disruption of natural microbial populations and dissemination into antibiotic resistant genes among microorganisms [3]. Among various antibiotics, tetracycline (TC) has been used in human and veterinary medicine and gradually become the second most widely used antibiotic around the world [4]. TC has a high aqueous solubility with a long environmental half-life [5] and

shown to disrupt microbial soil respiration [6], Fe(III) reduction [7] and nitrification [8]. This antibiotic is difficult to be metabolized and absorbed by the treated humans and animals; consequently, large fractions are excreted through urine and feces as an unmodified parent compound [9]. TC has determined in a number of samples, such as milk [10], plasma [11], pharmaceutical products [12] and water [13]. So far, various adsorbents including palygorskite [14], multi-walled carbon nanotubes (MWCNT) [15], aluminum and iron hydrous oxides [16], graphene oxide (GO) [17], silica [18], smectite clay [19], montmorillonite [20], chitosan particles [21], aluminum oxide [22], activated carbon (AC) [23], diatomite [24], polystyrene resins [25], boron nitride [26], metal ions impregnated polystyrene resins [27], Cu-13X [28] and molecularly imprinted polymer (MIP) [29] have studied for adsorption of pharmaceutical antibiotics in food and water samples.

Recently, the layered transition metal dichalcogenides (TMD) with the generic

formula  $\text{MX}_2$  have attracted much interest. In addition, the structure and general properties of pyrite-phase TMD ( $\text{FeS}_2$ ,  $\text{NiS}_2$  and  $\text{CoS}_2$ ) have been investigated [30–32]. Pyrite-phase TMD usually adopt the cubic pyrite structure and show interesting electronic, magnetic, and photo-voltaic properties. One important kind of TMD is cobalt sulfides including  $\text{CoS}_2$ ,  $\text{Co}_3\text{S}_4$ ,  $\text{CoS}$  and  $\text{Co}_9\text{S}_8$ , potentially applying in super capacitors, lithium-ion batteries, alkaline rechargeable batteries, magnetic materials and catalysts due to their excellent physical, chemical, electronic and optical properties [33–36]. In particular, cobalt disulfide ( $\text{CoS}_2$ ) has received considerable attention due to its metallic behavior [37].

Recently, there have been many studies on the  $\text{CoS}_2$ , due to the suitable properties for diversity of applications, such as dye-sensitized solar cells [38], lithium ion batteries [39] and super capacitors [40]. Nonetheless, the  $\text{CoS}_2$  has not employed as adsorbent till now. Appropriate adsorption features of synthesized the  $\text{CoS}_2$  is related to the surfaces of electrons rich which made it's as an appropriate candidate for the adsorption of polycyclic aromatic compounds like TC.

In this research, the  $\text{CoS}_2$  was structurally synthesized and morphologically characterized and used for the adsorption of tetracycline as a model analyte. The adsorbent has several attractive features compared to previous adsorbents including novelty, needless to pretreatment steps (such as modification and functionalization), numerous adsorption sites in surfaces, low cost synthesis, reusability and high recovery, which made it as an appropriate candidate for the adsorption of polycyclic aromatic compounds via  $\pi$ - $\pi$  interaction. The effect of various experimental parameters on the adsorption of antibiotic was investigated in batch adsorption experiments and the method was successfully employed for the adsorption of TC in agricultural water.

## 2. EXPERIMENTAL

### 2.1. Materials and Solutions

Tetracycline ( $\geq 95\%$  purity),  $\text{CoCl}_2 \cdot 6\text{H}_2\text{O}$ , thiourea and sodium chloride were obtained from Sigma Aldrich (chemical Co. Milwaukee, WI, USA). TC stock solution and other solutions were prepared in deionized water. The pH of solutions was adjusted by  $\text{NaOH}$  ( $0.1 \text{ mol L}^{-1}$ ) and  $\text{HCl}$  ( $0.1 \text{ mol L}^{-1}$ ).  $\text{HNO}_3$ ,  $\text{HCl}$  and  $\text{NaOH}$  (Merck, Darmstadt, Germany) were tested as eluent. The glassware were kept in acetone overnight and subsequently washed several times with deionized water before using.

### 2.2. Apparatus

A Perkin Elmer (Lambda 25, Perkin Elmer) spectrophotometer was used for UV-Vis spectra acquisition. The pH-meter model 692 from metrohm (Herisau, Switzerland) with combined glass electrode and a pH-indicator strips pH 0 - 14 Universal indicator from Merck were used for the pH measurements. A universal 320 R refrigerated centrifuge equipped with an angle rotor (6-place, 9000 rpm, Cat. No. 1620 A) was from Hettich (Kirchlengern, Germany). Surface morphology analysis of the adsorbent was carried out using a field emission scanning electron microscope, model S-4160 (procurement, Japan). For X-ray diffraction measurement, a Shimadzu 7000 S X-ray diffract meter with  $\text{Cu K}\alpha$  radiation ( $\lambda=1.54 \text{ \AA}$ ) was used. Energy dispersive X-ray (EDX) was performed by Oxford ED-2000 (England).

### 2.3. Hydrothermal Synthesis of the $\text{CoS}_2$

2 mmol  $\text{CoCl}_2 \cdot 6\text{H}_2\text{O}$  and 2 mmol thiourea and 60 mL of deionized water were mixture and put in 100 mL Teflon-coated autoclave at  $180 \text{ }^\circ\text{C}$  for 20 h. Then, the autoclave was cooled naturally to room temperature. The ultimate precipitates were centrifuged, washed with deionized water and absolute ethanol several times before dried in vacuum over 6 h at  $80 \text{ }^\circ\text{C}$ .

### 2.4. Sample collection and preparation

The water sample was analyzed immediately after preparation. Agricultural water was obtained from farmlands (kahak city, Iran). The collected water sample was filtered with filter paper, pH adjusted to 4 and the general procedure was carried out on. The TC concentration in the real sample was determined by UV-Vis spectrophotometry.

## 2.5. General Procedure

The batch experiments were carried out in 25 mL graduate falcon tubes containing the mixture of 20 mg adsorbent, 20% (w/v) NaCl and 20 mL TC aqueous solution ( $1 \text{ mgL}^{-1}$ ) with pH of 4. Conical bottom tubes were wrapped in aluminum foil to avoid possible photo degradation of tetracycline and was stirred for 20 min at ambient temperature in order to adsorption. After centrifuging of suspensions at 6000 rpm for 10 min and supernatant was decanted, 2 mL of  $0.2 \text{ mol L}^{-1} \text{ HNO}_3$  was used for desorption the TC which had remained on the  $\text{CoS}_2$  (shaking time: 5 min; centrifuging: 5 min). The amount of tetracycline in eluted solution was measured by UV-Vis spectrophotometer absorbance at 357.2 nm, using a calibration curve built with the antibiotics solution of different concentrations.

## 3. RESULT AND DISCUSSION

### 3.1. Characterization of $\text{CoS}_2$ Nanostructures

Figures 1A and B show the FESEM images of the  $\text{CoS}_2$  nanostructures. It was observed that the  $\text{CoS}_2$  particles have starfish-like architectures (Figure. 1A). The high magnification FESEM image (Figure. 1B) of the  $\text{CoS}_2$  shows the starfish-like architectures were composed by nanosheets. The XRD pattern of the products was shown in Figure. 1C. The peaks at  $2\theta = 28.04^\circ$ ,  $32.42^\circ$ ,  $35.76^\circ$ ,  $46.83^\circ$  and  $55.34^\circ$  were correlated to the (111), (200), (220), (211) and (311) plane of  $\text{CoS}_2$ , respectively, and all the diffraction peaks can be indexed to cubic  $\text{CoS}_2$  (JCPDS Card No. 41-1471). No other

cobalt sulfide impurities phases such as  $\text{Co}_3\text{S}_4$ ,  $\text{Co}_9\text{S}_8$ , and  $\text{CoS}$  were observed, indicating the prepared  $\text{CoS}_2$  has good crystallinity. The EDX of  $\text{CoS}_2$  (Figure. 1D) has analyzed, where the Co and S was the main element in this material.

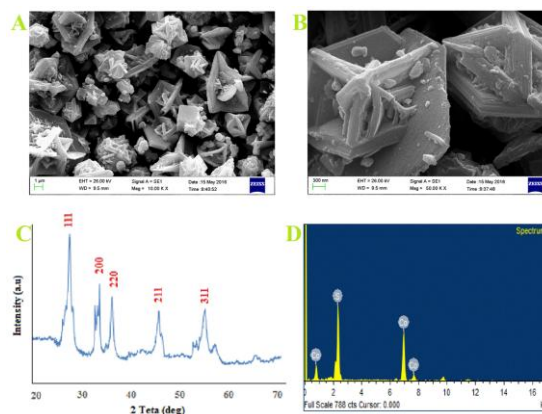


**Figure 1.** (A) FE-SEM image of the  $\text{CoS}_2$ , (B) the structure of sheets parallel of the  $\text{CoS}_2$ , (C) XRD pattern of  $\text{CoS}_2$  and (D) EDX image of the  $\text{CoS}_2$ .

### 3.2. Effect of pH

The influence of solution pH on adsorption of TC onto the  $\text{CoS}_2$  was studied in the pH range of 2–8. The results were shown in Figure. 2A. The removal of TC increased when the pH increased from 2 to around 4 to 5, and then decreased with further increasing pH from 6 to 8. This trend suggested that the adsorption of TC onto the adsorbent was strongly dependent on pH values and TC could be adsorbed with high percentage in range of pH 4-5. Therefore, pH of 4 was chosen as optimized pH.

The variation in pH can lead to a change in chemical speciation for ionizable organic compounds [41]. Tetracycline has several polar/ionizable groups, including amino, carboxyl, phenol, alcohol and ketone. It has three acid dissociation constants ( $\text{pK}_a = 3.3, 7.7$  and  $9.7$ ) and exists as a cationic, zwitterionic and anionic species under acidic, moderately acidic to neutral and alkaline conditions [42]. Specially, the amino group on the ring C4 has  $\text{pK}_a$  of 9.7 and is easily protonated

under favorable conditions. A  $\pi$ - $\pi$  interaction as dominant driving force has always used to explain the mechanism of aromatic adsorbate to the  $\text{CoS}_2$  surfaces. The  $\text{CoS}_2$  as a layered nanomaterial displays a maximum adsorption at 357.2 nm due to its  $\pi$ - $\pi$  transition. Moreover, as shown in Figure. 2A, the obviously decline of the recovery as  $\text{pH} < 4$  or  $\text{pH} > 6$  indicated that electrostatic interactions between TC and the  $\text{CoS}_2$  might also take place and affect the adsorption to a certain extent.

### 3.3. Effect of the adsorbent dose

The adsorbent dose is an important parameter since it determines the uptake capacity of a sorbent for a given analyte concentration under the operating conditions. The effect of adsorbent dose on the adsorption of TC was studied by varying the amount of the adsorbent within the range of 10-30 mg. The results are given in Figure. 2B. As expected, increasing the amount of adsorbent led to an increase in the percentage of the analyte adsorbed. The  $\text{CoS}_2$  has very high adsorption capacity; for a given concentration of analyte, an appropriate amount of adsorbent is enough and using more is not necessary. This may be due to the increased availability of surface active sites resulting from the increased dose and conglomeration of the adsorbent. The removal values for TC were found quantitative for an adsorbent amount of 20 mg. In all further studies, 20 mg  $\text{CoS}_2$  was used.

### 3.4. Effect of the Contact Time

The effect of shaking time was monitored by using the selected shaking time intervals 5-30 min and the antibiotic adsorption values were determined under the condition of pH 4. As the contact time increased, the adsorption gradually increased and then remained nearly constant after 20 min. The results (Figure. 2C) showed that the adsorption process should equilibrate for a sufficient time to

achieve the high adsorption percentage. In the present study 20 min was selected as the optimal adsorption time.

### 3.5. Desorption and Reusability

To ensure the complete elution of the target analyte from the adsorbent, desorption conditions should be studied. According to results for effect of pH, the adsorption of TC was not efficient in the strongly acidic aqueous media. Therefore, elution with acidic solution may be more favorable. As a result, different concentrations ( $1\text{-}3 \text{ mol L}^{-1}$ ) of various acids and base ( $\text{HNO}_3$ ,  $\text{HCl}$  and  $\text{NaOH}$ ) were employed to reuse the adsorbent. From the data given in Table 1, it is obvious that 2 mL of  $0.2 \text{ mol L}^{-1}$   $\text{HNO}_3$  could accomplish the quantitative elution of TC from the  $\text{CoS}_2$ .

The effect of desorption time of the analyte from the adsorbent after elution was also studied. It was found that 5 min was adequate for the complete recovery of the analyte. The relatively long desorption time may be attributed to the functional groups sensitive to pH in the antibiotic. Stability and reusability of the  $\text{CoS}_2$  was assessed through the performance of 5 cycles of adsorption and desorption under the optimized conditions. The results of Fig. 3 showed that the  $\text{CoS}_2$  was stable and reusable in the operation process (90-95%) without any significant loss of capacity and decrease in the recovery of the studied target analyte.

### 3.6. Effect of Salinity

Addition of inorganic salt may cause a modification of interaction between tetracycline and adsorbent. The ionic strength was adjusted by using  $\text{NaCl}$ . Different amounts of  $\text{NaCl}$  (0-30.0 % w/v) were added to the solution containing TC to investigate the effect of ion strength on the adsorption behavior. The results was shown in Fig. 2D. Taken as a whole, the general trend was evident and represented promotion effect. The percentage of removal increased to the addition of  $\text{NaCl}$

and after 20 % (w/v) NaCl reached an almost constant value.

The change of removal percentage with the addition of salt might result from the different contribution electrostatic interaction and of hydrophobic effect. The general improvement effect with addition of NaCl might mainly owing to the well-known salting out effect [43]. With addition of NaCl, the solubility of TC in water decreased and the decrease in solubility facilitated the diffusion of more TC to the surfaces of the adsorbent and increases adsorption capabilities. So the hydrophobic effect might be predominant in the adsorption. In pH 4, the adsorption increased monotonically with increasing  $\text{Na}^+$ , which was probably due to the fact that TC mainly existed as zwitterions at pH 4 and this zwitterions form made it hardly have electrostatic interactions with the  $\text{CoS}_2$ . It was thus deduced that besides hydrophobic effect, the electrostatic interactions between the analyte and the  $\text{CoS}_2$  also played an important role in the adsorption process.

### 3.7. Adsorption Kinetics

The experimental kinetic data of TC adsorption were correlated by pseudo first, second-order, intraparticle diffusion and Elovich models to study the rate and mechanism of adsorption. The experimental adsorption data at initial TC concentration of  $5 \text{ mg L}^{-1}$ , 20 % (w/v) NaCl and 20 mg of the  $\text{CoS}_2$  were examined and experimental data are presented in Table 2. These models can be represented with the following linear forms:

$$\log (q_e - q_t) = \log q_e - k_1 t/2.303 \quad (1)$$

$$t / q_t = 1/k_2 q_e^2 + t/q_e \quad (2)$$

$$q_t = k_i t^{1/2} + C \quad (3)$$

$$q_t = 1/\beta \ln (\alpha \beta) + 1/\beta \ln t \quad (4)$$

In the pseudo-first-order model plotting the values of  $\log (q_e - q_t)$  versus  $t$  may give a linear relationship [44]. Values of  $k_1$  and

$q_e$  were determined from the slope and intercept, respectively (Figure. 4A). Distance of intercept from experimental  $q_e$  value, indicates that this model was not suitable for fitting the experimental data. In pseudo second-order kinetic model [45], the plot of  $t/q_t$  versus  $t$  gives a straight line with high correlation coefficient. Constant  $k_2$  and equilibrium adsorption capacity ( $q_e$ ) were calculated from the intercept and slope of this line, respectively (Figure. 4B). The high values of  $r^2$  (0.99) strongly confirms the applicability of this model for explanation of adsorption kinetic data.

The intraparticle diffusion model relates between adsorption rate and square root of time ( $t$ ) [46]. The values of  $k_i$  and  $C$  were calculated from the slope and intercept of the plot of  $qt$  versus  $t_{1/2}$ .  $C$  value is related to the thickness of the boundary layer and  $k_i$  is the intraparticle diffusion rate constant ( $\text{mg g}^{-1} \text{ min}^{-1/2}$ ) were obtained from the final linear portion of above mention plot and presented in Table 2. Since, the intraparticle curve did not pass through the origin (Figure. 4C); one can notice that in addition to the intraparticle diffusion model another stage such as second order kinetic model control the adsorption process. The Elovich equation as another rate equation based on the adsorption capacity in linear form was applied for the adsorption of the antibiotic from an aqueous media [47]. The plot of  $q_t$  versus  $\ln t$  should yield a linear relationship with a slope and intercept of  $(1/\beta)$  and  $(1/\beta) \ln (\alpha \beta)$ , respectively. The Elovich constants obtained from the slope and the intercept of the straight line (Figure. 4D) are reported in Table 2. It is observed that the adsorption of TC followed more closely to pseudo second-order kinetics with regression coefficients  $> 0.99$  which fits the experimental data better than the other kinetic models for the entire adsorption process.

**Table 2.** Adsorption kinetics constants of TC on cobalt disulfide. Conditions: concentration;  $5 \text{ mg L}^{-1}$ , volume; 20 mL, ionic strength: 20 % w/v, dose of adsorbent; 20 mg.

Pseudo first order			Pseudo second order			Intraparticle			Elovich			
$q_e^{cal}$	$k_1$	$r^2$	$q_e^{cal}$	$k_2$	$r^2$	$k_i$	C	$r^2$	A	$\beta$	$r^2$	$q_{max}$
2.22	0.04	0.94	5.22	0.07	0.99	0.640	1.68	0.99	11.95	1.27	0.93	13.25

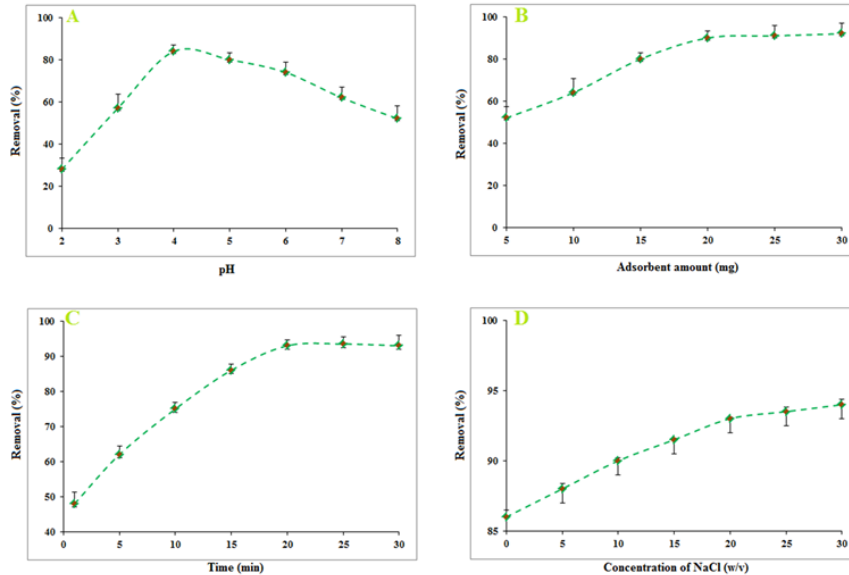


**Figure 2.** Effects of (A) pH (B) adsorbent dose (C) contact time and (D) ionic strength (NaCl) for TC adsorption onto the  $CoS_2$ .

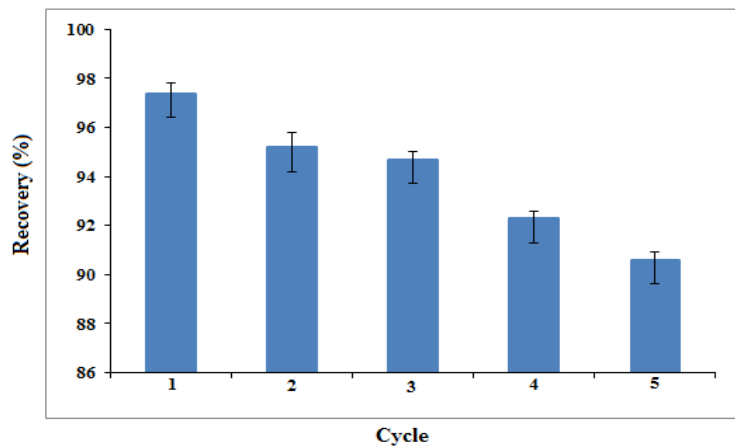


**Figure 3.** Reusability cycle of TC adsorption using the  $CoS_2$ .

**Table 3.** Adsorption isotherms parameters of Langmuir and Freundlich models for the adsorption of the TC on cobalt disulfide. Conditions: volume; 20 mL, pH; 4, contact time; 20 min, adsorbent; 20 mg; concentration: 5-100  $mg L^{-1}$ .

Langmuir			Freundlich		
$K_L(L mg^{-1})$	$q_{max} (mg g^{-1})$	$r^2$	$K_F$	$1/n$	$r^2$
0.0313	163.934	0.991	1.450	1.136	0.981

**Table 4.** Thermodynamic parameters for TC adsorption on cobalt disulfide. Conditions: volume; 20 mL, ionic strength: 20% w/v; contact time; 20 min, adsorbent; 20 mg, concentration; 5 mg L<sup>-1</sup>.

Thermodynamic parameters	283 K	293 K	303 K	313 K
$\Delta G^\circ$ (kJ/mol)	-5.275	-6.702	-7.417	-8.555
$\Delta H^\circ$ (kJ/mol)	24.584			
$\Delta S^\circ$ (J/mol K)	0.106			

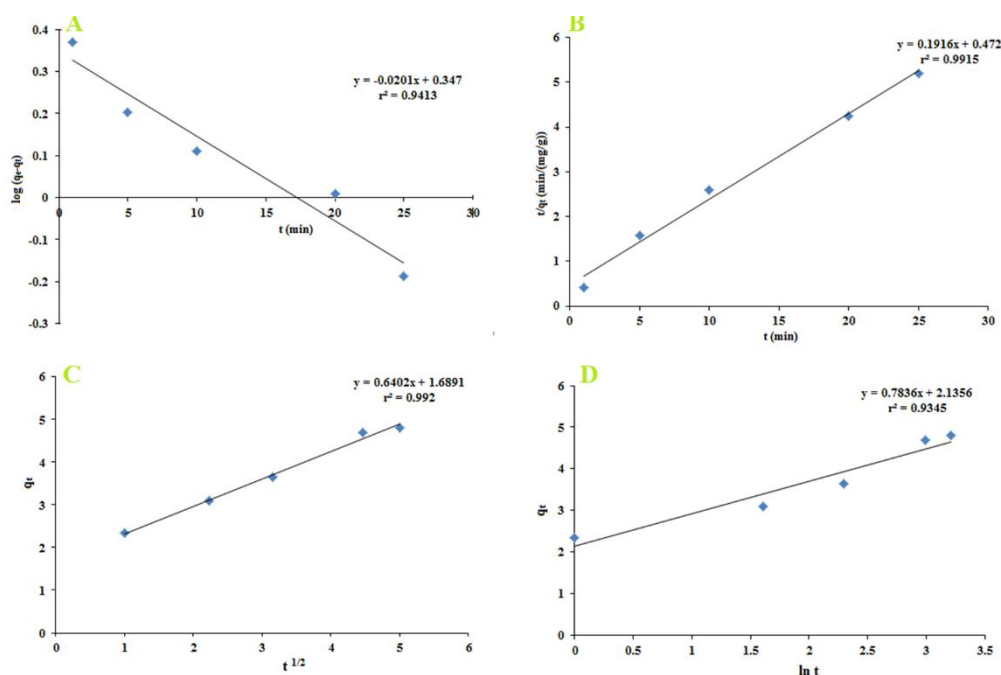


**Figure 4.** Kinetic plots for adsorption of TC on the CoS<sub>2</sub>. (A) Pseudo first order plot, (B) pseudo second order plot, (C) intraparticle plot and (D) Elovich plot.

### 3.8. Adsorption Isotherms

In order to gain a better understanding of adsorption mechanisms and evaluate the adsorption performance, the experimental data for TC adsorption onto the CoS<sub>2</sub> is analyzed using the Langmuir and Freundlich adsorption isotherm models. The pH of model solutions of 20 mL containing 5-100 mg L<sup>-1</sup> of TC was adjusted to 4 and was added to 20 mg adsorbent and 20 % (w/v) NaCl. The mixture was centrifuged, after shaking for 20 min. 2 mL of HNO<sub>3</sub> (0.2 mol L<sup>-1</sup>) of solution with eluent was analyzed by UV-Vis.

The adsorption data were fitted according to the linear form of the Langmuir isotherm model based on the following equation [48]:

$$C_e/q_e = (1/K_L q_m) + (C_e/q_m) \quad (5)$$

where  $q_e$  (mg g<sup>-1</sup>) is the equilibrium adsorption capacity,  $q_m$  (mg g<sup>-1</sup>) is the maximum amount of adsorbed analytes per unit weight of adsorbent to form complete monolayer coverage on the surface,  $C_e$  (mg.L<sup>-1</sup>) is the equilibrium concentration of analyte in aqueous solution and  $K_L$  (L.mg<sup>-1</sup>) represents enthalpy of sorption.

The Freundlich isotherm model represents properly the sorption process at low or intermediate concentration of analytes on a heterogeneous surfaces. It has the following equation [47]:

$$\log q_e = \log K_F + 1/n \log C_e \quad (6)$$

Where  $K_F$  ( $\text{mg}^{1-n} \text{L}^n \text{g}^{-1}$ ) and  $n$  are the Freundlich constant related to the adsorption capacity and adsorption intensity, respectively. The adsorption data were fitted according to the linear form of the Freundlich model.

Adsorption isotherms parameters of Langmuir and Freundlich models for the adsorption of the TC on the  $\text{CoS}_2$  at  $30^\circ\text{C}$  listed in Table 3. The adsorption isotherm fitted Langmuir model better than Freundlich model due to the larger correlation coefficient ( $r^2$ ), suggesting that TC adsorption on the  $\text{CoS}_2$  is monolayer chemical adsorption process [48].

Langmuir isotherm was used to determine the  $q_e$  and  $K_L$  values from the linear coefficients obtained by plotting  $C_e/q_e$  as a function of  $C_e$ . The adsorption capacity was found to be  $163.93 \text{ mg g}^{-1}$ . The Langmuir constant was  $0.031 \text{ L mg}^{-1}$ .

### 3.9. Adsorption Thermodynamic

The influence of temperature on TC adsorption was also conducted under different temperature from  $10$  to  $40^\circ\text{C}$ . According to the results, the temperature varying had little impact on the adsorption of TC.

The thermodynamic parameters were evaluated to confirm the nature of the adsorption and the inherent energetic changes involved during TC adsorption. Standard enthalpy ( $\Delta H^\circ$ ), free energy ( $\Delta G^\circ$ ) and entropy change ( $\Delta S^\circ$ ) were calculated to determine the thermodynamic feasibility and the spontaneous nature of the process. Therefore, the values of  $\Delta H^\circ$  and  $\Delta S^\circ$  were obtained from the slope and intercept of the  $\ln K_d$  versus  $1/T$  curve according to Eq. (7):

$$\ln K_d = \left(\frac{\Delta S^\circ}{R}\right) - \left(\frac{\Delta H^\circ}{RT}\right) \quad (7)$$

while the  $\Delta G^\circ$  value of can be determined from:

$$\Delta G^\circ = \Delta H^\circ - T\Delta S^\circ \quad (8)$$

where  $K_d$  ( $\text{L g}^{-1}$ ) is the distribution coefficient ( $K_d = q_e / C_e$ ),  $T$  (K) is the adsorption temperature and  $R$  ( $8.314 \text{ J mol}^{-1} \text{ K}^{-1}$ ) is the universal gas constant.

As shown in Table 4, the value of  $\Delta G^\circ$  for TC adsorption was negative at all temperatures, indicating that the adsorption of TC onto the  $\text{CoS}_2$  was spontaneous and thermodynamically feasible. The observed positive  $\Delta H^\circ$  and  $\Delta S^\circ$  values for TC adsorption suggested an endothermic process and increasing the temperature promoted the interaction between TC molecules and  $\text{CoS}_2$ .

### 3.10. Analysis of Environmental Water Sample

To investigate the environmental applicability of this method and its efficiency for TC uptake in various matrixes, an agricultural water with initial TC concentration of  $11.8 \text{ mg L}^{-1}$  (determined by HPLC) was analyzed according to the adsorption experiment. It was observed that about 88.3% of the antibiotic has removed from the sample which confirmed that the efficiency of the method is in good level for treatment of analyte in the real samples.

## 4. CONCLUSION

In this study, for the first time cobalt disulfide, was applied for adsorption of tetracycline antibiotic as a model analyte from polycyclic aromatic compounds. This adsorbent adsorbs polycyclic aromatic compounds by  $\pi$ - $\pi$  stacking. The main advantage of the  $\text{CoS}_2$  was its needless character to modification or functionalization, simple synthesis, reusability, environmentally friendly and numerous sulfur groups in surfaces in order to improve adsorption capacity. The Langmuir equation fitted the adsorption isotherm well. In conclusion, the proposed method reveals the great potential of the  $\text{CoS}_2$  as an advantageous adsorbent material. Although the obtained results of this research were related to the TC

adsorption, the system could be a considerable potential guide for the removal of other polycyclic aromatic compounds which are environmental pollutants.

## ACKNOWLEDGMENT

Support of this investigation by the Research Council of University of Tehran through grants is gratefully acknowledged.

## REFERENCES

1. Ji, L., Liu, F., Xu, Z., et al., (2010). "Adsorption of pharmaceutical antibiotics on template-synthesized ordered micro- and mesoporous carbons", *Environ Sci Technol.*, 44:3116–3122.
2. Eissen, M., Backhaus, D., (2011). "Pharmaceuticals in the environment: an educational perspective", *Environ Sci Pollut Res.*, 18: 1555–1566.
3. Paseban, N., Ghadam, P., Pourhosseini, PS., (2019). "The Fluorescence Behavior and Stability of AgNPs Synthesized by Juglans Regia Green Husk Aqueous Extract", *Int. J. Nanosci Nanotechnol.*, 15: 117–126.
4. Sun, H., Shi, X., Mao, J., Zhu, D., (2010). "Tetracycline sorption to coal and soil humic acids: an examination of humic structural heterogeneity", *Environ Toxicol Chem.*, 29: 1934–1942.
5. Dudhane, A. A., Waghmode, SR., Dama, LB., et al., (2019). "Synthesis and Characterization of Gold Nanoparticles using Plant Extract of Terminalia arjuna with Antibacterial Activity", *Int. J. Nanosci Nanotechnol.*, 15: 75–82.
6. Thiele. Bruhn, S., (2003). "Pharmaceutical antibiotic compounds in soils a review", *J. Plant Nutr Soil Sci.*, 166: 145–167.
7. Li, Z., Schulz, L., Ackley, C., Fenske, N., (2010). "Adsorption of tetracycline on kaolinite with pH-dependent surface charges", *J. Colloid Interface Sci.*, 351: 254–260.
8. Boleas, S., Alonso, C., Pro, J., et al., (2005). "Toxicity of the antimicrobial oxytetracycline to soil organisms in a multi-species-soil system and influence of manure co-addition", *J. Hazard Mater.*, 122: 233–241.
9. Thiele. Bruhn, S., Beck, I. C., (2005). "Effects of sulfonamide and tetracycline antibiotics on soil microbial activity and microbial biomass", *Chemosphere*, 59: 457–465.
10. Halling. Sørensen, B., (2001). "Inhibition of aerobic growth and nitrification of bacteria in sewage sludge by antibacterial agents", *Arch Environ Contam Toxicol.*, 40: 451–460.
11. Ji, L., Chen, W., Bi, J., et al., (2010). "Adsorption of tetracycline on single-walled and multi-walled carbon nanotubes as affected by aqueous solution chemistry", *Environ Toxicol Chem.*, 29: 2713–2719.
12. Furusawa, N., (2003). "Isolation of tetracyclines in milk using a solid-phase extracting column and water eluent", *Talanta.*, 59: 155–159.
13. Rudek, M. A., March, CL., Bauer, K. S., et al., (2000). "High-performance liquid chromatography with mass spectrometry detection for quantitating COL-3, a chemically modified tetracycline, in human plasma", *J. Pharm Biomed Anal.*, 22: 1003–1014.
14. Monser, L., Darghouth, F., (2000). "Rapid liquid chromatographic method for simultaneous determination of tetracyclines antibiotics and 6-epi-doxycycline in pharmaceutical products using porous graphitic carbon column", *J. Pharm Biomed Anal.*, 23: 353–362.
15. Wang, Y., Xu, X., Han, J., Yan, Y., (2011). "Separation/enrichment of trace tetracycline antibiotics in water by [Bmim] BF<sub>4</sub> (NH<sub>4</sub>)<sub>2</sub>SO<sub>4</sub> aqueous two-phase solvent sublation", *Desalination.* 266: 114–118.
16. Chang, P. H., Li, Z., Yu, T. L., et al., (2009). "Sorption removal of tetracycline from water by palygorskite", *J. Hazard Mater.*, 165: 148–155.
17. Zhang, L., Song, X., Liu, X., et al., (2011). "Studies on the removal of tetracycline by multi-walled carbon nanotubes", *Chem Eng J.*, 178: 26–33.
18. Gu, C., Karthikeyan, K. G., (2005). "Interaction of tetracycline with aluminum and iron hydrous oxides", *Environ Sci Technol.*, 39: 2660–2667.
19. Gao, Y., Li, Y., Zhang, L., et al., (2012). "Adsorption and removal of tetracycline antibiotics from aqueous solution by graphene oxide", *J Colloid Interface Sci.*, 368: 540–546.
20. Turku, I., Sainio, T., Paatero, E., (2007). "Thermodynamics of tetracycline adsorption on silica", *Environ Chem Lett.*, 5: 225–228.
21. Li, Z., Chang, P. H., Jean, J. S., et al., (2010). "Interaction between tetracycline and smectite in aqueous solution", *J. Colloid Interface Sci.*, 341: 311–319.
22. Wang, Y. J., Jia, D. A., Sun, R. J., et al., (2008). "Adsorption and cosorption of tetracycline and copper (II) on montmorillonite as affected by solution pH", *Environ Sci Technol.*, 42: 3254–3259.
23. Caroni, A., De, Lima. CRM, Pereira. MR, Fonseca J. L. C., (2009). "The kinetics of adsorption of tetracycline on chitosan particles", *J. Colloid Interface Sci.*, 340: 182–191.
24. Chen, W. R., Huang, C. H., (2010). "Adsorption and transformation of tetracycline antibiotics with aluminum oxide", *Chemosphere*, 79: 779–785.

25. Choi, K. J., Kim, S. G., Kim, S. H., (2008). "Removal of antibiotics by coagulation and granular activated carbon filtration", *J. Hazard Mater.*, 151: 38–43.
26. Chao, Y., Zhu, W., Chen, F., et al., (2014). "Commercial diatomite for adsorption of tetracycline antibiotic from aqueous solution", *Sep Sci Technol.*, 49: 2221–2227.
27. Chao, Y., Zhu, W., Yan, B., et al., (2014). "Macro porous polystyrene resins as adsorbents for the removal of tetracycline antibiotics from an aquatic environment", *J. Appl. Polym. Sci.*, 131: 1–8.
28. Chao, Y., Zhu, W., Chen, J., et al., (2014). "Development of novel graphene-like layered hexagonal boron nitride for adsorptive removal of antibiotic gatifloxacin from aqueous solution", *Green. Chem. Lett. Rev.*, 7: 330–336.
29. Chao, Y., Zhu, W., Ye, Z., et al., (2015). "Preparation of metal ions impregnated polystyrene resins for adsorption of antibiotics contaminants in aquatic environment", *J. Appl. Polym. Sci.*, 132: 1 - 9.
30. Lv, J. M., Ma, Y. L.; Chang, X., Fan, S. B., (2015). "Removal and removing mechanism of tetracycline residue from aqueous solution by using Cu-13X", *Chem. Eng. J.*, 273: 247–253.
31. Sánchez. Polo, M; Velo, Gala, I., López-Peñalver, J. J., Rivera. Utrilla, J., (2015). "Molecular imprinted polymer to remove tetracycline from aqueous solutions", *Microporous Mesoporous Mater.*, 203: 32–40.
32. Wang, D. W., Wang, Q. H., Wang, T. M., (2010). "Controlled growth of pyrite FeS<sub>2</sub> crystallites by a facile surfactant-assisted solvothermal method", *Cryst. Eng. Comm.*, 12: 755–761.
33. Kong, D., Cha, J. J., Wang, H., et al., (2013). "First-row transition metal dichalcogenide catalysts for hydrogen evolution reaction", *Energy Environ Sci.*, 6: 3553–3558.
34. Kong, D., Wang, H., Lu, Z., Cui, Y., (2014). "CoSe<sub>2</sub> nanoparticles grown on carbon fiber paper: an efficient and stable electrocatalyst for hydrogen evolution reaction", *J. Am. Chem. Soc.*, 136: 4897–4900.
35. Mahmood, N., Zhang, C., Jiang, J., et al., (2013). "Multifunctional Co<sub>3</sub>S<sub>4</sub>/graphene composites for lithium ion batteries and oxygen reduction reaction", *Chem. Eur. J.*, 19: 5183–5190.
36. Chen, H. W; Kung, C. W., Tseng, C. M., et al., (2013). "Plastic based dye-sensitized solar cells using Co<sub>9</sub>S<sub>8</sub> acicular nanotube arrays as the counter electrode", *J. Mater. Chem. A.*, 1: 13759–13768.
37. Gu, Y., Xu, Y; Wang, Y., (2013). "Graphene-wrapped CoS nanoparticles for high-capacity lithium-ion storage", *ACS Appl. Mater. Interfaces*, 5: 801–806.
38. Tang, J., Shen, J., Li, N., Ye, M., (2014). "A free template strategy for the synthesis of CoS<sub>2</sub>-reduced graphene oxide nanocomposite with enhanced electrode performance for supercapacitors", *Ceram. Int.*, 40: 15411–15419
39. Faber, MS; Dziedzic, R., Lukowski, M. A., et al., (2014). "High-performance electrocatalysis using metallic cobalt pyrite (CoS<sub>2</sub>) micro- and nanostructures", *J. Am. Chem. Soc.*, 136: 10053–10061.
40. Bi, E., Chen, H., Yang, X., et al., (2014). "A quasi core-shell nitrogen-doped graphene/cobalt sulfide conductive catalyst for highly efficient dye-sensitized solar cells", *Energy Environ Sci.*, 7: 2637–2641.
41. Yan, J. M., Huang, HZ; Zhang, J., et al., (2005). "A study of novel anode material CoS<sub>2</sub> for lithium ion battery", *J. Power Sources.*, 146: 264–269.
42. Xing, J. C., Zhu, Y. L., Zhou, Q. W., et al., (2014). "Fabrication and shape evolution of CoS<sub>2</sub> octahedrons for application in supercapacitors", *Electrochim Acta.*, 136: 550–556.
43. Van Doorslaer, X., Demeestere, K., Heynderickx, P. M., et al., (2011). "UV-A and UV-C induced photolytic and photocatalytic degradation of aqueous ciprofloxacin and moxifloxacin: reaction kinetics and role of adsorption", *Appl. Catal. B. Environ.*, 101: 540–547.
44. Li, B., Zhang, T., (2013). "Removal mechanisms and kinetics of trace tetracycline by two types of activated sludge treating freshwater sewage and saline sewage", *Environ Sci. Pollut. Res.*, 20: 3024–3033.
45. Yang, W., Lu, Y., Zheng, F., et al., (2012). "Adsorption behavior and mechanisms of norfloxacin onto porous resins and carbon nanotube", *Chem. Eng. J.*, 179: 112–118.
46. Karimi, M. A., Ghasemi, M. H., Aghagoli, M. J., Beyki, M. H., (2016). "Preconcentration of cobalt ions by a melamine-modified cellulose@MWCNT nanohybrid", *Microchim Acta.*, 183: 2949–2955.
47. Beyki, M. H., Bayat, M., Shemirani, F., (2016). "Fabrication of core-shell structured magnetic nanocellulose base polymeric ionic liquid for effective biosorption of Congo red dye", *Bioresour Technol.*, 218:326–334. <https://doi.org/10.1016/j.biortech.2016.06.069>.
48. Beyki, M. H., Feizi, F., Shemirani, F., (2016). "Melamine-based dendronized magnetic polymer in the adsorption of Pb(II) and preconcentration of rhodamine B", *React Funct Polym.*, 103:81–91. <https://doi.org/10.1016/j.reactfunctpolym.2016.04.006>.
49. Beyki, M. H., Bayat, M., Miri, S., et al., (2014). "Synthesis, characterization, and silver adsorption property of magnetic cellulose xanthate from acidic solution: Prepared by one step and biogenic approach", *Ind Eng Chem Res.*, 53:14904–14912. <https://doi.org/10.1021/ie501989q>.
50. Hossein Beyki, M., Shirkhodaie, M., Karimi, M. A; et al., (2016). "Green synthesized Fe<sub>3</sub>O<sub>4</sub> nanoparticles as a magnetic core to prepare poly 1, 4 phenylenediamine nanocomposite: employment for fast adsorption of lead ions and azo dye", *Desalin. Water. Treat.*, 57: 1–12.